Miscibility in Cross-Linked Polymer−Solvent Systems with Nematic Interactions

Farida Benmouna,[†] Ulrich Maschke,*[,‡] Xavier Coqueret,[‡] and Mustapha Benmouna[†]

Institut of Chemistry, University Aboubakr Belkaïd, Bel Horizon, BP119, 13000 Tlemcen, Algeria; and Laboratoire de Chimie Macromoléculaire, Bâtiment C6, CNRS UPRESA No. 8009, Université des Sciences et Technologies de Lille, 59655 Villeneuve d'Ascq Cedex, France

Received April 7, 1999; Revised Manuscript Received October 25, 1999

ABSTRACT: Model phase diagrams of cross-linked polymers and low molecular weight solvent systems with nematic interactions are discussed. A combination of classical theories of network elasticity due to cross-links, isotropic mixing with solvent, and a nematic interaction of the Maier−Saupe type yields a variety of phase behaviors. The network elasticity parameters and the Flory−Huggins interaction parameter are assumed to be function of the volume fraction in contrast to our previous studies of analogous systems. Effects of nematic order on the miscibility of cross-linked polymers and low molecular weight LC are discussed by comparison with the corresponding isotropic systems. The case of side chain liquid crystal cross-linked networks and isotropic solvents is also examined within the same theoretical scheme. The influence of cross-linking density and the reference polymer volume fraction at cross-linking on the phase behavior is also invoked.

1. Introduction

Problems related with the miscibility of polymer−solvent systems with nematic interactions are the subject of growing interest. The primary motivation for this particular attention is due to the potential applications of these systems in various fields such as digital displays, computers, privacy windows and so on.[1−3] Mixing high molecular weight polymers and low molecular weight solvents in the presence of both isotropic and anisotropic interactions gives rise to fascinating phase properties which have attracted the curiosity of many research groups for more than 2 decades. It is not our pretention to review all the studies reported in the literature on this subject, but we have made a biased selection of few papers on linear and cross-linked polymers that are most relevant to our present study.

One of the early studies of the phase behavior of linear polymers and nematic solvents was reported by Kronberg et al.[4] These authors were interested in the curvature of the phase boundaries in the temperature/composition plane upon heating and cooling. They analyzed these curvatures with a simple theory in which the isotropic part of the chemical potential is given by the Flory−Huggins model while the nematic part is related to the heat of the nematic−isotropic transition for the liquid crystal (LC) in the pure state. They introduced two Flory−Huggins interaction parameters χ_i and χ_n depending on whether the monomer interacts with the LC in its isotropic or nematic state, respectively. A similar investigation was considered by Dubault et al.[5]

Ballauff[6−8] discussed the phase equilibria occurring in mixtures of linear polymers and nematic LCs using the Flory lattice model. Anisotropic forces between LC rodlike molecules are also described using the Flory lattice model. Both isotropic−isotropic (I−I) and isotropic−nematic coexisting phases are obtained within this theory. The I−I demixing takes place if the power of the LC as a solvent is low enough. A three-phase equilibrium emerges below which a nematic phase coexists with an isotropic phase having a high polymer content.

A theoretical formalism of polymers and LCs was put forward by Brochard[9] for non nematogenic polymers and generalized to mixtures of side chain LC polymers (SCLCP) and low molecular weight liquid crystals (LMWLC) by Brochard et al.[10] This theory is based on a combination of the Flory−Huggins model of isotropic mixing and the Maier−Saupe model of nematic order. It accommodates for different characteristics of the two nematogens, and in particular, the nematic−isotropic transition temperatures of the two components are allowed to be different. A variety of phase diagrams are obtained by changing the length of the polymer. Kyu and co-workers generalized this theory to the case of LMWLC having both a smectic−nematic transition and a nematic−isotropic transition[11,12] and to mixtures of nematogens for which the cross-nematic quadrupole interaction parameter is not equal to the square root of the product of the parameters for pure nematogens.[13]

Although simple, these models are found to be very useful for the interpretation of experimental phase diagrams obtained by optical microscopy, light scattering, and differential scanning calorimetry.[12,14]

Phase equilibria of cross-linked polymer networks and LMWLC were also investigated by several authors. Ballauff[15] developed a theory of swelling equilibria of networks in nematogen solvents combining the Flory lattice theory with the Flory−Rehner model for the elastic free energy of the network. His main concern was on the degree of swelling of the isotropic network in a nematic LC.

Warner and Wang[16] calculated the phase diagrams of cross-linked polymers with SCLC groups swollen by isotropic solvents. Later, they generalized this work to the case of nematogen mixtures.[17]

* To whom correspondence should be addressed (e-mail: maschke@univ-lille1.fr).
[†] University Aboubakr Belkaïd.
[‡] Université des Sciences et Technologies de Lille.

10.1021/ma990517z CCC: $19.00
Published on Web 01/14/2000

Boots et al. examined both theoretically[18] and experimentally[19] the swelling of isotropic cross-linked polymers by LMWLC. They were interested in the phase separation during cross-linking and polymerization process.

Matsuyama et al.[20] considered the volume phase transition of cross-linked polymers and LMWLC using a combination of the Flory−Rehner and the Maier−Saupe theories. Second-order volume phase transitions were found at the nematic−isotropic transition temperature of the pure LC phase.

Recently, we reported a comparative study of the equilibrium phase behavior of isotropic polymers and nematic LC considering the case of cross-linked and linear polymers.[21] Binodal curves and the spinodal extension of the unstable regions were calculated in both polymer architectures. The case where the LMWLC exhibits both a smectic A−nematic and a nematic−isotropic transition temperature was also considered within a Maier−Saupe−McMillan theory of anisotropic interactions.[22] In refs 21 and 22, it was assumed that the Flory−Huggins interaction parameter was a function of temperature only and that the elasticity parameters were constant properties. To our knowledge, no phase diagram is reported at present where these parameters are functions of the polymer concentration for systems exhibiting nematic order.

In the present paper, a theoretical investigation of the equilibrium phase diagram of several systems showing a nematic order is presented assuming that both the Flory−Huggins interaction parameter and the rubber elasticity parameters of the cross-linked network are functions of the polymer concentration.

The elasticity parameters α and β are model dependent, and their values are the subject of controversial arguments in the literature. It is beyond the scope of this work to discuss these controversies. The choice made here (see eq 2) is intermediate between the original Flory−Wall model of suppressed fluctuations of cross-links where $\alpha = 1$ and $\beta = 2/f$, and the phantom network model of free fluctuations of cross-links where $\alpha = (f - 2)/f$ and $\beta = 0$.

Recent data describing the phase behavior of electron beam cured propoxylated glycerol triacrylate/8CB systems[23] have shown that the choice of α and β in eq 2 is suitable for data interpretation of the phase diagram of cross-linked polymers and LMWLC. This observation does not mean that the classical models of cross-links fluctuations (affine, phantom, etc....), where α and β are constant, fail completely, but it only means that the present choice may be useful as an alternative model of data analysis. Combining these α and β values with the Flory−Huggins interaction parameter given in eqs 3 and 4, it was possible to achieve a good agreement between theory and experiments for the system investigated in ref 23.

This controversial choice of the model for rubber elasticity illustrates the complexity of the phase diagrams of cross-linked polymers and LC as compared to linear polymer systems. There are other subtilities related with the presence of defects in the network such as pendent chains, trapped entanglements, loops, etc. whose discussion is clearly beyond this paper. Here, we consider the idealized homogeneous network with a constant cross-linking density represented by a constant number of repeat units between consecutive cross-links. This hypothesis leads to serious inaccuracies which need to be addressed for a better understanding of the phase diagrams of cross-linked polymers and LMWLC and possible discrepancies between experimental data and simple theoretical models such as the one presented here.

Although the phase behavior of cross-linked polymers swollen by isotropic solvents is well documented in the literature[24−31] it is reconsidered here for the purpose of introducing notations and definitions. This part is essentially inspired from refs 30 and 31.

2. Equilibrium Phase Properties of Isotropic Mixing

2.1. The Free Energy. The equilibrium phase properties of isotropic systems made of linear or cross-linked polymers and low molecular weight solvents is a well-documented problem in the literature.[24,25] In the case of linear polymers, the interplay between entropic forces favoring mixing and strong enthalpic repulsions driving the system toward phase separation can be described quite well within the Flory−Huggins lattice model.[24] For a cross-linked polymer network, the existence of chemical cross-links imposes elastic bounds onto swelling of the polymer and modifies substantially the phase behavior.[26] To examine this problem in more detail, the following free energy density is used

$$\frac{f^{(i)}}{k_B T} = \frac{F^{(i)}}{n_t k_B T} = \frac{3\alpha\varphi_0^{2/3}}{2N_c}[\varphi_2^{1/3} - \varphi_2] + \frac{\beta\varphi_2}{N_c}\ln\varphi_2 + \frac{\varphi_1 \ln\varphi_1}{N_1} + \chi\varphi_1\varphi_2 \quad (1)$$

The symbol F represents the free energy for the whole system while f is the free energy density; k_B is the Boltzmann constant and T the absolute temperature. The superscript i refers to the isotropic part of the free energy. Later, we shall use the superscript n for the nematic part. The subscripts 1 and 2 designate solvent and polymer, respectively. n_1 is the number of solvent molecules and n_2 is the number of repeat units in the network. N_1 is the volume ratio of solvent molecules and monomeric building block of the polymer such that the total volume can be expressed as a number of repeat units $n_t = n_1 N_1 + n_2$. φ_1 and φ_2 are the volume fractions of components 1 and 2, respectively, satisfying the incompressibility condition $\varphi_1 = 1 - \varphi_2 = n_1 N_1/n_t$; For simplicity, it will be assumed that all units occupy the same reference volume ($N_1 = 1$). φ_0 is the volume fraction of polymer at cross-linking. If polymer cross-linking takes place in the bulk, then $\varphi_0 = 1$ otherwise φ_0 has values between 0 and 1.

The cross-linking density of the network is described by the average number of monomers between two consecutive cross-links denoted N_c. The rubber elasticity parameters α and β appearing in the free energy of eq 1 are model dependent. They can have constant values or depend on polymer volume fraction. Here, we choose the latter option and let[27−31]

$$\alpha = \frac{f - 2 + 2\varphi_2}{f}, \quad \beta = \frac{2\varphi_2}{f} \quad (2)$$

where f is the monomer functionality. Finally, the Flory−Huggins interaction parameter χ, which governs the miscibility of the isotropic system, is assumed to be

function of temperature and composition according to

$$\chi = \chi_0 + \chi_1\varphi_2 + \chi_2{\varphi_2}^2 \tag{3}$$

where χ_0 depends on temperature only

$$\chi_0 = A + \frac{B}{T} \tag{4}$$

The numerical constants A and B are sometimes used as adjustable parameters to obtain the best fit with the experimental data.[11,13,32]

Variation of the Flory−Huggins interaction parameter with various quantities such as the polymer concentration has been a subject of a long debate in the literature arousing a particular interest for a long time[33] and still continues to be a question of controversial arguments.[34] A detailed discussion of this important question is beyond the scope of the present work but few remarks are in order. Koningsveld and co-workers[35,36] were probably among the ones that considered this question in the greatest details. They reported a systematic study of liquid−liquid-phase separation in multicomponent polymer systems and copolymers. Considering poly(styrene)/cyclohexane data they came to the conclusion that these data are best fitted with the form $\chi = 0.2035 + (90.55/T) + 0.3091\varphi_2 + 0.1554{\varphi_2}^2$.[35]

Van Emmerik and Smolders[37] studied the equilibrium phase behavior of solutions of poly(dimethylphenyleneoxide) and toluene using light scattering, and their data analysis required an interaction parameter to be function of polymer concentration. Benoît et al.[38] proposed an expansion of the interaction parameter with the polymer concentration using the chain of contacts model at increasing orders. Their qualitative argument was meant to relate the interaction parameters by light scattering to those obtained by other techniques such as osmometry. More recently Moerkerke et al.[30,31] considered the phase equilibria of poly(*N*-isopropylacrylamide) in water considering solutions with either cross-linked or linear polymers. They analyzed their data assuming that the Flory−Huggins interaction parameter varies with the polymer concentration according to $\chi = \chi_0 + \chi_1\varphi_2 + \chi_2{\varphi_2}^2$.

2.2. Chemical Potentials. Binodals describe the composition of the phases in equilibrium. This is obtained by solving the set of equations expressing the equality of chemical potentials μ_1 and μ_2 in the coexisting phases. The latter are given by differentiating the free energy with respect to the number of molecules n_1 and n_2. In the isotropic case, one has

$$\mu_1^{(\mathrm{i})} = \left(\frac{\partial F^{(\mathrm{i})}}{\partial n_1}\right)_{n_2} \tag{5}$$

$$\mu_2^{(\mathrm{i})} = \left(\frac{\partial F^{(\mathrm{i})}}{\partial n_2}\right)_{n_1} \tag{6}$$

which can be written in terms of $f^{(\mathrm{i})}$ and its derivative with respect to φ_2

$$\frac{\mu_1^{(\mathrm{i})}}{N_1} = f^{(\mathrm{i})} - \varphi_2\frac{\mathrm{d}f^{(\mathrm{i})}}{\mathrm{d}\varphi_2} \tag{7}$$

$$\mu_2^{(\mathrm{i})} = f^{(\mathrm{i})} - \varphi_1\frac{\mathrm{d}f^{(\mathrm{i})}}{\mathrm{d}\varphi_1} \tag{8}$$

Differentiating eq 1 with respect to φ_2 yields

$$\frac{1}{k_{\mathrm{B}}T}\frac{\mathrm{d}f^{(\mathrm{i})}}{\mathrm{d}\varphi_2} = \frac{{\varphi_0}^{2/3}}{N_{\mathrm{c}}}\left\{\frac{\alpha}{2}({\varphi_2}^{-2/3} - 3) + \frac{3{\varphi_2}^{1/3}}{\mathrm{f}}(1 - {\varphi_2}^{2/3})\right\} + \frac{\beta + (\beta + 2\varphi_2/\mathrm{f})\ln\varphi_2}{N_{\mathrm{c}}} - \frac{\ln\varphi_1 + 1}{N_1} + \chi_0(1 - 2\varphi_2) + \chi_1\varphi_2(2 - 3\varphi_2) + \chi_2{\varphi_2}^2(3 - 4\varphi_2) \tag{9}$$

When two isotropic phases (a) and (b) are in equilibrium, the volume fraction $\varphi_1^{(\mathrm{a})}$ and $\varphi_1^{(\mathrm{b})}$ are obtained by solving the set of equations

$$\mu_1^{(\mathrm{ia})} = \mu_1^{(\mathrm{ib})} \tag{10}$$

$$\mu_2^{(\mathrm{ia})} = \mu_2^{(\mathrm{ib})} \tag{11}$$

Using eqs 7−11 yields

$$f^{(\mathrm{i})} - \varphi_2\frac{\mathrm{d}f^{(\mathrm{i})}}{\mathrm{d}\varphi_2}\bigg|^a = f^{(\mathrm{i})} - \varphi_2\frac{\mathrm{d}f^{(\mathrm{i})}}{\mathrm{d}\varphi_2}\bigg|^b \tag{12}$$

$$\frac{\mathrm{d}f^{(\mathrm{i})}}{\mathrm{d}\varphi_2}\bigg|^a = \frac{\mathrm{d}f^{(\mathrm{i})}}{\mathrm{d}\varphi_2}\bigg|^b \tag{13}$$

2.3. Isotropic Spinodals. Transitions from metastable to unstable regions are given by the spinodal equations obtained by letting $\partial^2 f/\partial{\varphi_2}^2 = 0$. Differentiating eq 9 yields

$$\frac{1}{k_{\mathrm{B}}T}\frac{\partial^2 f^{(\mathrm{i})}}{\partial{\varphi_2}^2} = \frac{{\varphi_0}^{2/3}}{N_{\mathrm{c}}}\left\{-\frac{\alpha}{3{\varphi_2}^{5/3}} + \frac{2}{\mathrm{f}{\varphi_2}^{2/3}} - \frac{6}{\mathrm{f}}\right\} + \frac{4(\ln\varphi_2 + 1)}{\mathrm{f}N_{\mathrm{c}}} + \frac{\beta}{N_{\mathrm{c}}\varphi_2} + \frac{1}{N_1\varphi_1} - 2\{\chi_0 + \chi_1(3\varphi_2 - 1) + 3\chi_2\varphi_2(2\varphi_2 - 1)\} = 0 \tag{14}$$

2.4. Phase Diagrams. A typical phase diagram is given in Figure 1 where we have used

$$N_1 = 1; \quad N_{\mathrm{c}} = 10^3; \quad \varphi_0 = 0.25; \quad \mathrm{f} = 3 \tag{15}$$

and

$$\chi_0 = -0.35 + \frac{342}{T}; \quad \chi_1 = 0.3; \quad \chi_2 = 0.04 \tag{16}$$

The value of $N_{\mathrm{c}} = 10^3$ corresponds to a low cross-linking density while $\varphi_0 = 0.25$ implies that cross-linking takes place at the polymer volume fraction of 0.25.

The variation of χ_0 with temperature gives rise to a phase diagram showing an upper critical solution temperature (UCST) while the values of χ_1 and χ_2 are typical for poly(styrene)/cyclohexane and similar systems.[35,36] The solid curve is the binodal while the dashed curve represents the spinodal. The critical point can be obtained by solving in addition to eq 14, the following eq $\partial^3 f^{(\mathrm{i})}/\partial{\varphi_2}^3 = 0$ which yields explicitly

$$\frac{{\varphi_0}^{2/3}}{N_{\mathrm{c}}}\left\{\frac{5\alpha}{9{\varphi_2}^{8/3}} - \frac{2}{\mathrm{f}{\varphi_2}^{5/3}}\right\} + \frac{6}{\mathrm{f}N_{\mathrm{c}}\varphi_2} - \frac{\beta}{N_{\mathrm{c}}{\varphi_2}^2} + \frac{1}{N_1{\varphi_1}^2} - 6\{\chi_1 + \chi_2(4\varphi_2 - 1)\} = 0 \tag{17}$$

The procedure of deriving the phase equilibria of swollen and collapsed network phases in the isotropic state was

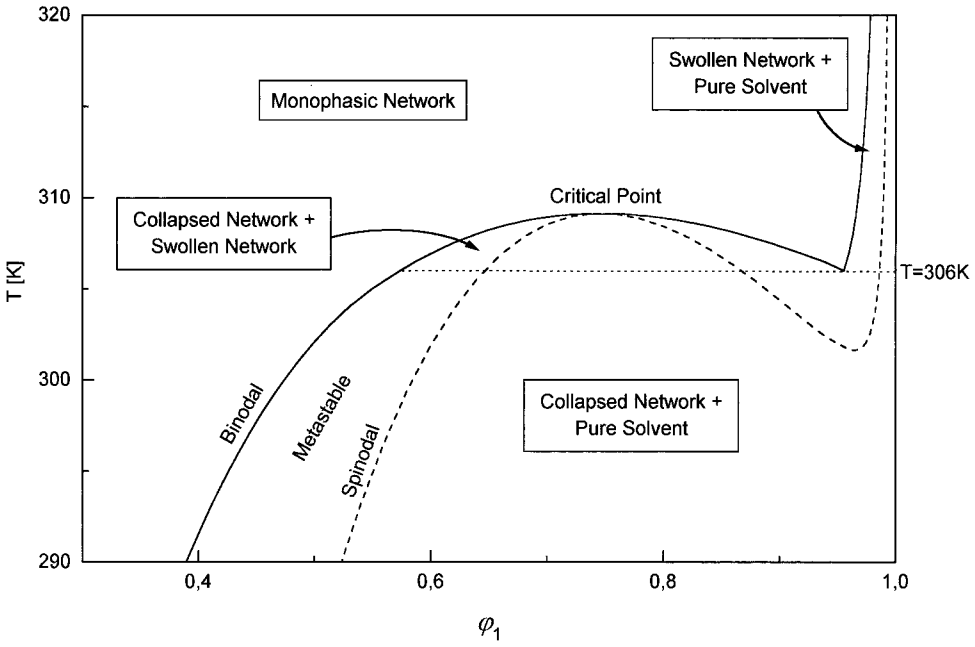

Figure 1. Phase diagram of an isotropic system made of a cross-linked polymer and a solvent. The solid line is the binodal and the dashed line is the spinodal. The phases are indicated on the diagram. The parameters used to plot this diagram are as follows: $\chi = \chi_0 + \chi_1\varphi_2 + \chi_2\varphi_2^2$ (Flory−Huggins interaction parameter); $\chi_0 = -0.35 + (342/T)$; $\chi_1 = 0.3$; $\chi_2 = 0.04$; $\alpha = ((f - 2 + 2\varphi_2)/f)$, $\beta = (2\varphi_2/f)$ (network elasticity parameters); $f = 3$ (functionality of monomers at cross-links); $\varphi_0 = 0.25$ (polymer volume fraction at cross-linking); $N_1 = 1$ (number of repeat units of solvent); $N_c = 10^3$ (number of repeat units between two cross-links).

described in detail by Moerkerke et al.[30] Apart from differences in the notations, eqs 14 and 17 are identical to eqs 9a and 9b of ref 30.

Therefore, similar observations can be made concerning the solutions of these eqs and in particular the emergence of two critical points and the conditions of their stability. The reader is referred to this paper for more details on this question. Here we content ourselves with few remarks relevant for our discussion later when the effects of nematic interactions are included. One observes that the phase diagram is divided into two distinguished parts. In the upper part, the network/solvent system forms a single phase of a swollen or a collapsed network depending upon temperature and polymer volume fraction. The upturn of the binodal curve in the right-hand side (rhs) of the diagram is a characteristic feature of cross-linked polymers. Below the solid curve, the phase diagram is divided into several regions of coexisting phases. The horizontal dotted line indicates a temperature ($T = 34$ °C) at which three phases are in equilibrium: a swollen network, a collapsed network, and a pure solvent phase. Above this temperature, on the rhs of the diagram, a swollen network is in equilibrium with a pure solvent phase. In the region between the solid curve and the dotted line, a network miscibility gap appears whereby a swollen network is in equilibrium with a collapsed network. The interaction polymer−solvent χ is such that a strong interfacial tension exists between a dense and a more dilute polymer phase within the network itself. Below the dotted line, the phase diagram shows a region where a collapsed network is in equilibrium with a pure solvent phase. All these regions show standard phase properties satisfying the Gibbs phase rule, and similar results were reported by Moerkerke et al.[30,31]

Changes in the cross-linking density lead to substantial modifications as one can see from Figure 2 which corresponds to a higher cross-linking density (i.e., $N_c = 10^2$). On the left-hand side (lhs) of the solid line, there is a single network phase with a variable degree of swelling. On the rhs of this line, a swollen network is in equilibrium with a pure solvent phase. For such a high cross-linking density, the miscibility gap of the network and the three-phase equilibrium are not obtained. Increasing the cross-linking density results into a larger separation between the spinodal and the binodal curves. For the system under consideration with the particular choice of parameters used to plot this diagram, it was found that the occurrence of two network phases disappears for concentration independent values of α and β. This result seems to be in discrepancy with the observation made by Moerkerke et al.[30] according to which the phase diagram obtained with α and β given by eq 2 is very similar to that corresponding to $\alpha = 1$ and $\beta = 0$.

3. Cross-linked Polymers and Nematic Liquid Crystals

3.1. Nematic Free Energy and Order Parameter. The equilibrium phase behavior of mixtures of cross-linked polymers and nematic LC has been examined by various authors before.[14,16−19,21,22]

In addition to the isotropic part of eq 1, one has a contribution which describes the nematic order. Within the Maier−Saupe theory,[39,40] the nematic free energy is given by

$$\frac{f^{(n)}}{k_B T} = \frac{F^{(n)}}{n_t k_B T} = \varphi_1\left[-\ln Z_1 + \frac{1}{2}\nu_{11}\varphi_1 s_1^2\right] \quad (18)$$

s_1 is the nematic order parameter of the LC

$$s_1 = \frac{1}{2}[3\langle\cos^2\theta\rangle - 1] \quad (19)$$

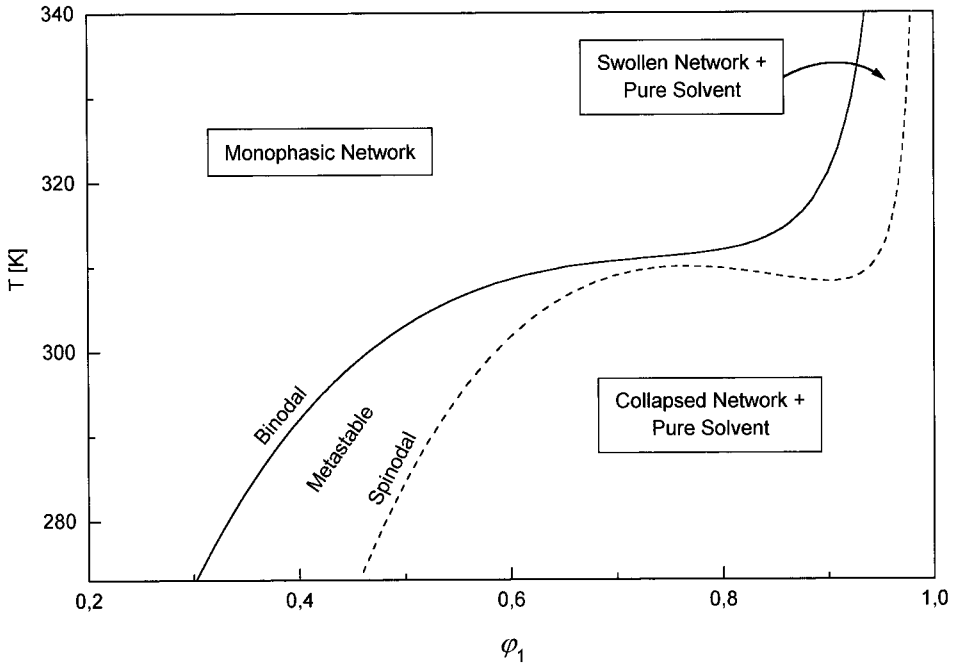

Figure 2. Same parameters as Figure 1 with $N_c = 10^2$.

θ is the angle between a reference axis and the director of the LC; the symbol $\langle ... \rangle$ represents the average with respect to the orientational distribution function

$$\psi^{(n)}(\mu) = \frac{e^{-U_1(\mu)/(k_B T)}}{Z_1}; \quad \mu \equiv \cos\theta \tag{20}$$

$U_1(\mu)$ is the orientational potential

$$\frac{U_1(\mu)}{k_B T} = -\frac{m_1}{2}[3\mu^2 - 1] \tag{21}$$

where m_1 is a mean field parameter representing the potential strength. Minimization of the nematic free energy with respect to s_1 yields

$$m_1 = \varphi_1 \nu_{11} s_1 \tag{22}$$

where ν_{11} is the Maier−Saupe quadrupole interaction parameter

$$\nu_{11} = 4.54\frac{T_{NI\,1}}{T} \tag{23}$$

$T_{NI\,1}$ is the nematic−isotropic transition temperature of the LC. Z_1 represents the nematic partition function

$$Z_1 = \int e^{-U_1(\mu)/(k_B T)}\, d\mu \tag{24}$$

Combining eqs 19, 21, and 24 yields

$$s_1 = -\frac{\partial}{\partial m_1}\ln Z_1 \tag{25}$$

3.2. Nematic Chemical Potentials. The nematic chemical potentials are given by similar derivatives as in eqs 5 to 8 replacing the superscript (i) by (n). Combining these results with eq 18 yields

$$\frac{\mu_1^{(n)}}{N_1 k_B T} = -\ln Z_1 + \frac{\nu_{11}\varphi_1^{\,2} s_1^{\,2}}{2} \tag{26}$$

$$\frac{\mu_2^{(n)}}{k_B T} = \frac{\nu_{11}\varphi_1^{\,2} s_1^{\,2}}{2} \tag{27}$$

The nematic contribution to the spinodal equation is given by the second derivative of the free energy

$$\frac{1}{k_B T}\frac{\partial^2 f^{(n)}}{\partial \varphi_2^{\,2}} = \frac{\partial}{\partial \varphi_2}\ln Z_1 \tag{28}$$

Combining this with eqs 22 and 25 yields

$$\frac{1}{k_B T}\frac{\partial^2 f^{(n)}}{\partial \varphi_2^{\,2}} = -\nu_{11} s_1\left[s_1 + \varphi_1\frac{ds_1}{d\varphi_1}\right] \tag{29}$$

Letting $(d^2 f^{(i)}/d\varphi_2^{\,2}) + (d^2 f^{(n)}/d\varphi_2^{\,2}) = 0$, one obtains the spinodal equation in the explicit form

$$\frac{\varphi_0^{\,2/3}}{N_c}\left\{\frac{-\alpha}{3\varphi_2^{\,5/3}} + \frac{2}{f\varphi_2^{\,2/3}} - \frac{6}{f}\right\} + \frac{4(\ln\varphi_2 + 1)}{fN_c} + \frac{\beta}{N_c\varphi_2} + \frac{1}{N_1\varphi_1} - 2\{\chi_0 + \chi_1(2\varphi_2 - 1) + 6\chi_2\varphi_2(2\varphi_2 - 1)\} - \nu_{11} s_1\left[s_1 + \varphi_1\frac{ds_1}{d\varphi_1}\right] = 0 \tag{30}$$

Figure 3 represents the phase diagram of a cross-linked polymer and a monomeric LC with $T_{NI\,1} = 60$ °C. The value of $T_{NI\,1}$ has been taken to be equal to the experimental value obtained for E7, a commercially available nematic LC mixture containing essentially cyanobiphenylene derivatives. The remaining parameters are the same as in Figure 1. The thick dashed line gives the limiting volume fraction of LC $\varphi_{NI\,1}$ below which the nematic order parameter s_1 is zero. This line separates the spinodal curve into two branches. Unlike

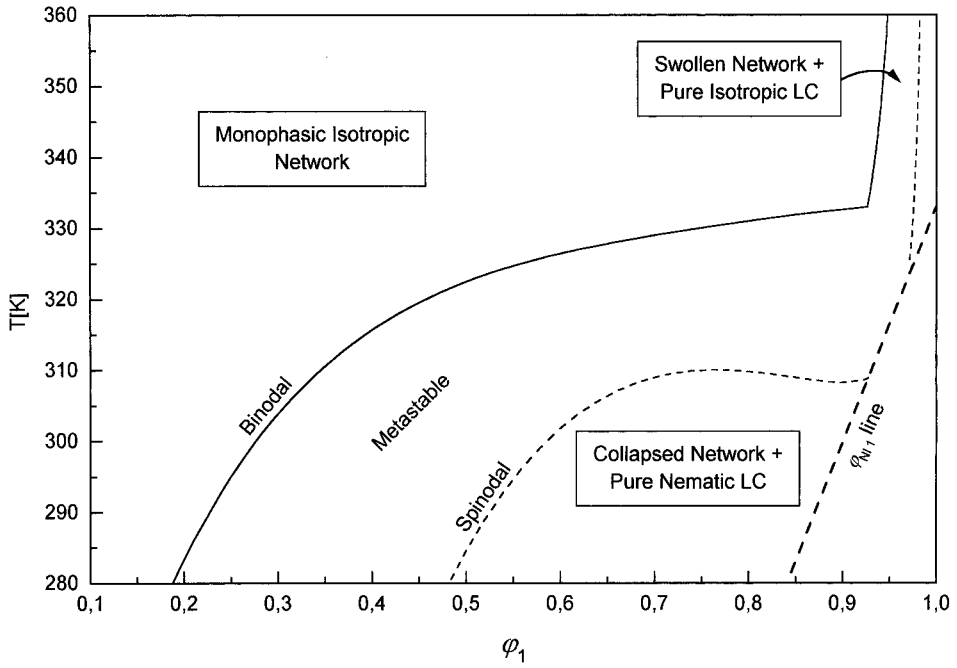

Figure 3. Same parameters as Figure 1 with a nematic−isotropic transition temperature $T_{NI\,1}$ = 60 °C.

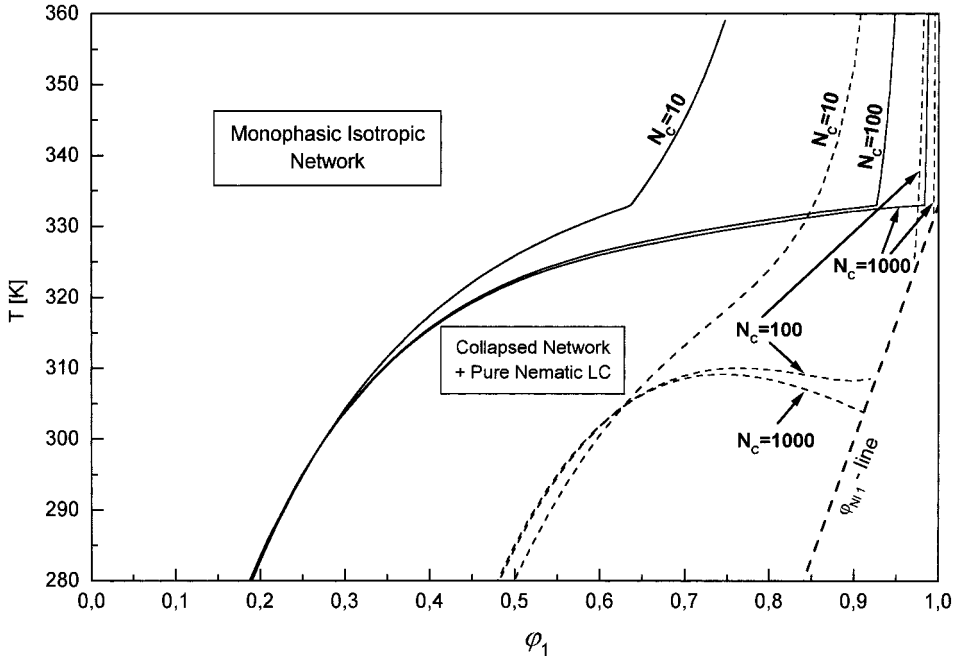

Figure 4. Same parameters as Figure 3 with three values of N_c as indicated on the diagrams. This figure illustrates the effects of the cross-linking density on the miscibility of this system.

the case of linear polymers, the spinodal equation does not admit a solution above $\varphi_{NI\,1}$, and hence the nematic branch does not exist.

Essentially, two distinct parts are found in this diagram. On the lhs of the solid curve one has a monophasic network/solvent system in the isotropic state. On the rhs of the solid line, one has two distinct regions. Below the transition temperature $T_{NI\,1}$, an isotropic polymer/solvent phase (a) is in equilibrium with a pure LC phase in the nematic order (b). Since $\varphi_1^{(b)} = 1$, the composition of phase (a) is obtained simply by solving the equation $\mu_1^{(ia)} = 0$. Above $T_{NI\,1}$, a swollen isotropic network coexists with a pure LC in its isotropic state. The polymer volume fraction of the swollen network is also obtained by solving the equation $\mu_1^{(ia)} = 0$. Comparing this diagram with Figure 1 reveals that the tendency toward phase separation of the network−solvent system originally due to the isotropic parameter χ is enhanced in the presence of nematic interactions.

Clearly, the cross-linking density has a strong influence on the miscibility gap. This is shown in Figure 4 which collects the phase diagrams for $N_c = 10^3$, 10^2, and 10 while the $\varphi_{NI\,1}$ line is independent of N_c. The area of the biphasic region below $T_{NI\,1}$ and the solid curve is slightly increased when N_c decreases. Above $T_{NI\,1}$, on

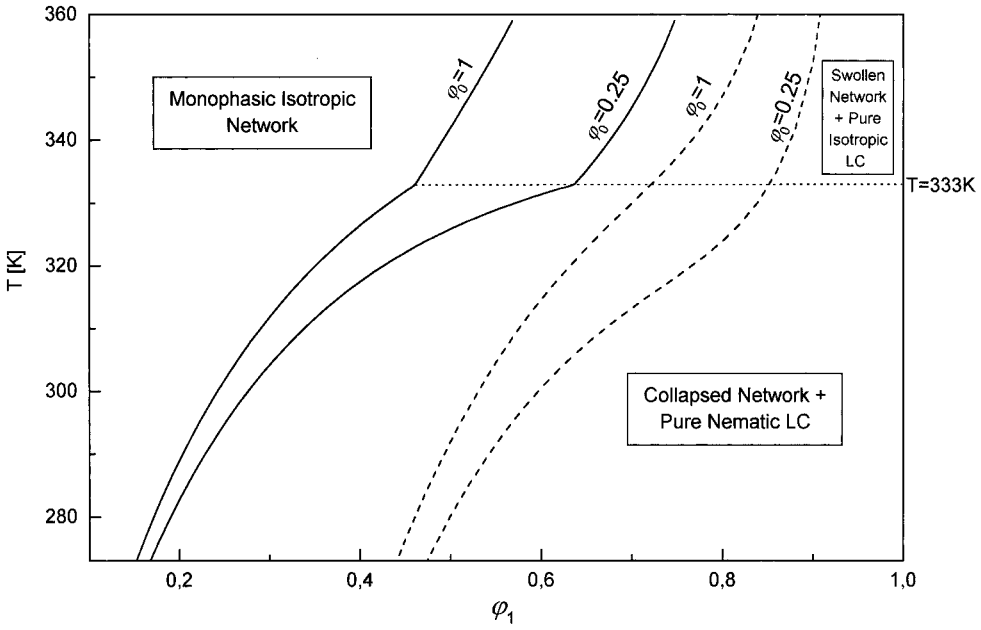

Figure 5. Same parameters as Figure 4 with $N_c = 10$ and two values of φ_0 as indicated on the curves.

the rhs of the solid line, the isotropic miscibility gap is substantially extended in the case of dense networks. This behavior is illustrated by the phase diagrams corresponding to $N_c = 10^3$ and 10^2. One notes that the spinodal of the system with $N_c = 10$ crosses the other two dashed lines at $T = 32$ °C. This means that below this temperature, the unstable region is slightly enlarged when the cross-linking density increases and N_c goes from 10^2 to 10. The miscibility gap as indicated by the continuous curve does not change significantly with the value of N_c below 32 °C (305 K). The reason for which the unstable region is slightly broadened in this range of N_c is not yet clear to us.

The influence of the volume fraction at cross-linking φ_0 on the miscibility of the system depends on the density of cross-links in the network. Theoretical phase diagrams were established using $\varphi_0 = 1$ and 0.25 for three cross-linking densities corresponding to $N_c = 10^3$, 10^2, and 10. We found that for the highest two values of N_c the nematic + isotropic biphasic region is practically the same with $\varphi_0 = 0.25$ and 1. Only the part of the phase diagram above $T_{NI\,1}$ is slightly shifted to the left when N_c decreases from 10^3 to 10^2. For $N_c = 10$, the miscibility gap is much more extended when φ_0 increases from 0.25 to 1. Figure 5 illustrates this effect quite clearly for $N_c = 10$ and the two values of φ_0. For $\varphi_0 = 1$, the diagram shifts to the left, leading to a wide miscibility gap. Phase separation between polymer and LC takes place at a lower polymer content when the network is cross-linked in the bulk.

4. Side Chain Liquid Crystal cross-linked Polymers and Isotropic Solvents

The phase behavior of SCLCP with cross-links and isotropic solvents is quite different from that of the previous system. Grafting of the mesomorphic groups to the polymer backbone results into profound changes in the phase behavior. First, the nematic−isotropic transition temperature may change substantially because of coupling between side chain nematic groups and the polymer backbone. The nematic free energy has a form similar to eq 18 with the subscript 1 changed into 2:

$$\frac{f^{(n)}}{k_B T} = \frac{F^{(n)}}{n_t k_B T} = \varphi_2\left[-\ln Z_2 + \frac{1}{2}\nu_{22}\varphi_2 {s_2}^2\right] \quad (31)$$

Clearly, similar definitions hold for Z_2, s_2, and ν_{22} as in the previous case exchanging the subscripts 1 and 2. The nematic−isotropic transition for this system is designated by $T_{NI\,2}$. Likewise, the derivative of the free energy needed in the calculation of chemical potentials involves the new partition function Z_2

$$\frac{df^{(n)}}{d\varphi_2} = -\ln Z_2 \quad (32)$$

Recalling that eqs 7 and 8 can be applied to the nematic chemical potentials, one obtains

$$\frac{\mu_1^{(n)}}{N_1 k_B T} = \frac{\nu_{22}{\varphi_2}^2 {s_2}^2}{2} \quad (33)$$

$$\frac{\mu_2^{(n)}}{k_B T} = -\ln Z_2 + \frac{\nu_{22}{\varphi_2}^2 {s_2}^2}{2} \quad (34)$$

According to eq 32 the second derivative of the nematic free energy is

$$\frac{\partial^2 f^{(n)}}{\partial {\varphi_2}^2} = -\frac{\partial}{\partial \varphi_2}\ln Z_2 \quad (35)$$

Recalling that $s_2 = -(\partial/\partial m_2)\ln Z_2$ and $m_2 = \varphi_2\nu_{22}s_2$, one arrives at

$$\frac{\partial^2 f^{(n)}}{\partial {\varphi_2}^2} = -\nu_{22}s_2\left[s_2 + \varphi_2\frac{ds_2}{d\varphi_2}\right] \quad (36)$$

The calculation of the binodal (solid curve) and the resolution of the spinodal equation $\partial^2 f/\partial {\varphi_2}^2 = 0$ (dashed

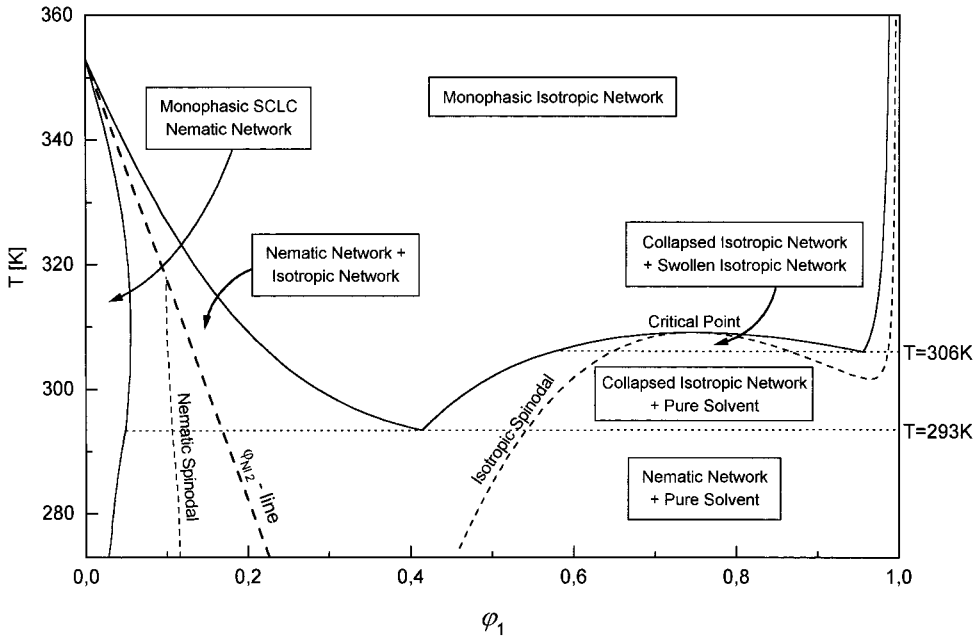

Figure 6. Same parameters as Figure 1 with a SCLC cross-linked polymer having a nematic−isotropic transition temperature $T_{NI\,2} = 80$ °C.

curve) are illustrated in Figure 6 for $N_c = 10^3$ and $\varphi_0 = 0.25$. Unlike the preceding cases, the spinodal here presents both isotropic and nematic branches. The thick dashed line gives the volume fraction $\varphi_{NI\,2}$ below which the nematic interaction vanishes and the nematic branch of the spinodal stops. In the upper part of this figure above the solid curve, there is a monophasic region where the polymer and the solvent form a single isotropic phase. The upturn of the binodal characteristic of cross-linked polymers at high solvent composition is also present here due to the elastic bounds imposed by the cross-links and leading to the emergence of a pure solvent phase in equilibrium with a swollen network.

The lower part of the diagram presents several regions of different phase properties. On the lhs, one has a single nematic phase of the SCLC with a small amount of solvent. Below $T = 20$ °C (lower horizontal dotted line), a nematic polymer rich phase (a) coexists with a pure solvent isotropic phase (b). Since $\varphi_1^{(b)} = 1$, the composition of the polymer rich phase is given by solving the equation $\mu_1^{(ia)} + \mu_1^{(na)} = 0$. Between $T = 20$ °C and $T = 33$ °C (upper horizontal dotted line), a collapsed isotropic network (a) is in equilibrium with a pure solvent phase (b). Given that $\varphi_1^{(b)} = 1$, the composition of the swollen network is found simply by solving the equation $\mu_1^{(ia)} = 0$. On the lhs of the diagram a network miscibility gap exists where a nematic phase is in equilibrium with an isotropic phase. The composition of these phases are obtained by solving the set of equations

$$f - \varphi_2 \frac{\partial f}{\partial \varphi_2}\bigg|^a = f^{(i)} - \varphi_2 \frac{\partial f^{(i)}}{\partial \varphi_2}\bigg|^b \tag{37}$$

$$\frac{\partial f}{\partial \varphi_2}\bigg|^a = \frac{\partial f^{(i)}}{\partial \varphi_2}\bigg|^b \tag{38}$$

with $f = f^{(i)} + f^{(n)}$. Between the dotted horizontal line at 33 °C and the solid curve, there is another network miscibility gap where a collapsed (a) and a swollen network (b) are in equilibrium. Both phases are isotropic and their compositions are found by solving the set of equations

$$f^{(i)} - \varphi_2 \frac{\partial f^{(i)}}{\partial \varphi_2}\bigg|^a = f^{(i)} - \varphi_2 \frac{\partial f^{(i)}}{\partial \varphi_2}\bigg|^b \tag{39}$$

and

$$\frac{\partial f^{(i)}}{\partial \varphi_2}\bigg|^a = \frac{\partial f^{(i)}}{\partial \varphi_2}\bigg|^b \tag{40}$$

Conclusions

The effects of nematic interactions on the miscibility of cross-linked polymers and low molecular weight solvent molecules are investigated from the theoretical point of view. Phase diagrams of systems made of isotropic polymer networks and low molecular weight LC solvents show a large gap of miscibility as compared to analogous systems without nematic order. This prediction was made keeping the same thermodynamic parameters and letting the nematic−isotropic transition temperature for the LC to be equal to 60 °C characteristic of the eutectic mixture known as E7. The miscibility gap increases with the cross-linking density and with the reference volume fraction φ_0 at which cross-linking of the polymer takes place. The calculations show that the loss of miscibility due to increasing φ_0 is significant only in the high cross-linking density. The spinodal extension of the unstable region admits only an isotropic branch. Unlike the case of linear polymer systems, the spinodal equation does not admit a solution for LC composition above φ_{NI}, implying the absence of the nematic branch from the diagram. SCLC cross-linked polymer networks and isotropic solvents show a completely different phase behavior. The fact that the nematogen groups are grafted on the polymer backbone leads to a change in the nematic−isotropic transition temperature and a different miscibility in the temperature/composition plane. To illustrate these features, we

select a system in which the nematic−isotropic transition temperature is $T_{NI\,2} = 80$ °C. A single nematic phase is found at high polymer contents. A three phase equilibrium is found: a nematic dense polymer, an isotropic swollen polymer and a pure solvent. Another three phase equilibrium is obtained at high solvent contents: A collapsed network, a swollen network, and a pure solvent phase. For these systems, the spinodal exhibits two branches: an isotropic branch in the dilute polymer region and a nematic branch in the concentrated polymer range.

Phase equilibria of nematogen mixtures with SCLC cross-linked polymers and nematic LC are the subject of a separate work.[41]

References and Notes

(1) Doane, J. W. Polymer Dispersed Liquid Crystal Displays. In *Liquid Crystals: Their Applications and Uses*, Bahadur, B.; Ed.; World Scientific: Singapore, 1990.
(2) Drzaic, P. S. *Liquid Crystal Dispersions*; World Scientific: Singapore, 1995.
(3) Maschke, U.; Coqueret, X.; Loucheux, C. *J. Appl. Polym. Sci.* **1995**, *56*, 1547.
(4) Kronberg, B.; Bassignana, I.; Patterson, D. *J. Phys. Chem.* **1978**, *82*, 1714.
(5) Dubault, A.; Casagrande, C.; Veyssie, M. *Mol. Cryst. Liq. Cryst. Lett.* **1982**, *72*, 189.
(6) Ballauff, M. *Ber. Bunsen-Ges. Phys. Chem.* **1986**, *90*, 1053.
(7) Ballauff, M. *Mol. Cryst. Liq. Cryst.* **1986**, *136*, 175.
(8) Ballauff, M. *Mol. Cryst. Liq. Cryst. Lett.* **1986**, *4*, 15.
(9) Brochard, F. *C. R. Hebd. Seances Acad. Sci.* **1979**, *289B*, 229.
(10) Brochard, F.; Jouffroy, J.; Levinson, P. *J. Phys. (Paris)* **1984**, *45*, 1125.
(11) Shen, C.; Kyu, T. *J. Chem. Phys.* **1995,** *102*, 556.
(12) Chiu, H.-W.; Kyu, T. *J. Chem. Phys.* **1995**, *103*, 7471.
(13) Chang, M.-C.; Chiu, H.-W.; Wang, X. Y.; Kyu, T.; Leroux, N.; Campbell, S.; Chien, L.-C. *Liq. Cryst.* **1998**, *25*, 733.
(14) Finkelmann, H.; Kock, H. J.; Rehage, G. *Mol. Cryst. Liq. Cryst.* **1982**, *89*, 23.
(15) Ballauff, M. *Mol. Cryst. Liq. Cryst.* **1991**, *196*, 47.
(16) Warner, M.; Wang, X.-J. *Macromolecules* **1992**, *25*, 445.
(17) Wang, X.-J.; Warner, M. *Macromol. Theory Simul.* **1997**, *6*, 37.
(18) Boots, H. M. J.; Kloosterboer, J. G.; Serbutoviez, C.; Touwslager, F. J. *Macromolecules* **1996**, *29*, 7683.
(19) Serbutoviez, C.; Kloosterboer, J. G.; Boots, H. M. J.; Touwslager, F. J. *Macromolecules* **1996**, *29*, 7690.
(20) Matsuyama, A.; Morii, R.; Kato, T. *Mol. Cryst. Liq. Cryst.* **1998**, *312*, 117.
(21) Benmouna, F.; Bedjaoui, L.; Maschke, U.; Coqueret, X.; Benmouna, M. *Macromol. Theory Simul.* **1998**, *7*, 599.
(22) Benmouna, F.; Coqueret, X.; Maschke, U.; Benmouna, M. *Macromolecules* **1998**, *31*, 4879.
(23) Maschke, U.; Benmouna, F.; Roussel, F.; Daoudi, A.; Gyselinck, F.; Buisine, J.-M.; Coqueret, X.; Benmouna, M. *Macromolecules* **1999**, *32*, 8866.
(24) Flory, P. J. *Principles of Polymer Chemistry*; Cornell University Press: Ithaca, NY, 1965.
(25) Mark, J. E.; Erman, B. *Rubberlike Elasticity−A Molecular Primer*; John Wiley: New York, 1988.
(26) Dusek, K. *J. Polym. Sci. C* **1967**, *16*, 1289.
(27) Flory, P. J.; Erman, B. *Macromolecules* **1982**, *15*, 800.
(28) Petrovic, Z. S.; MacKnight, W. J.; Koningsveld, R.; Dusek, K. *Macromolecules* **1987**, *20*, 1088.
(29) Mishra, V.; Du Prez, F. E.; Gosen, E.; Goethals, E. J.; Sperling, L. H. *J. Appl. Polym. Sci.* **1995**, *58*, 331.
(30) Moerkerke, R.; Koningsveld, R.; Berghmans, H.; Dusek, K.; Solc, K. *Macromolecules* **1995**, *28*, 1103.
(31) Moerkerke, R.; Meeussen, F.; Koningsveld, R.; Berghmans, H.; Mondelaers, W.; Schacht, E.; Dusek, K.; Solc, K. *Macromolecules* **1998**, *31*, 2223.
(32) Shen, C. Ph.D. Dissertation, University of Akron, Akron, OH, 1995.
(33) Tompa, H. *Polymer Solutions*, Butterworth: London, 1956.
(34) Benoît, H. *C. R. Hebd. Seances Acad. Sci., Ser. IIb* **1999**, *327*, 139.
(35) Koningsveld, R.; Staverman, A. J. *J. Polym. Sci., Part A2* **1968**, *6*, 325.
(36) Koningsveld, R.; Kleintjens, L. A.; Shultz, A. R. *J. Polym. Sci., Part A2* **1970**, *8*, 1261.
(37) Van Emmerik, P. T.; Smolders, C. A. *J. Polym. Sci., Part C* **1972**, *39*, 311.
(38) Benoît, H.; Strazielle, C.; Benmouna, M. *Acta Polym.* **1988**, *39*, 75.
(39) Maier, W.; Saupe, A. *Z. Naturforsch.* **1959**, *14a*, 882.
(40) Maier, W.; Saupe, A. *Z. Naturforsch.* **1960**, *15a*, 287.
(41) Benmouna, F.; Maschke, U.; Coqueret, X.; Benmouna, M. *J. Polym. Sci., Polym. Phys. Ed.*, in press.

MA990517Z